environmental microbiology

Environmental Microbiology (2021) **23**(8), 4726–4740 doi:10.1111/1462-2920.15681

Functional dissection of the phosphotransferase system provides insight into the prevalence of *Faecalibacterium prausnitzii* in the host intestinal environment

Deborah Kang,[†] Hyeong-In Ham,[†] Seung-Hwan Lee, Yong-Joon Cho, Yeon-Ran Kim, Chang-Kyu Yoon[*] and Yeong-Jae Seok[*]

School of Biological Sciences and Institute of Microbiology, Seoul National University, Seoul, 08826, Republic of Korea.

Summary

***Faecalibacterium prausnitzii* is a dominant member of healthy human colon microbiota, regarded as a beneficial gut bacterium due to its ability to produce anti-inflammatory substances. However, little is known about how *F. prausnitzii* utilizes the nutrients present in the human gut, influencing its prevalence in the host intestinal environment. The phosphoenolpyruvate (PEP):carbohydrate phosphotransferase system (PTS) is a widely distributed and highly efficient carbohydrate transport system found in most bacterial species that catalyses the simultaneous phosphorylation and import of cognate carbohydrates; its components play physiological roles through interaction with other regulatory proteins. Here, we performed a systematic analysis of the 16 genes encoding putative PTS components (2 enzyme I, 2 HPr, and 12 enzyme II components) in *F. prausnitzii* A2-165. We identified the general PTS components responsible for the PEP-dependent phosphotransfer reaction and the sugar-specific PTS components involved in the transport of two carbohydrates, *N*-acetylglucosamine and fructose, among five enzyme II complexes. We suggest that the dissection of the functional PTS in *F. prausnitzii* may help to understand how this species outcompetes other bacterial species in the human intestine.**

Received 22 March, 2021; revised 20 June, 2021; accepted 19 July, 2021. *For correspondence. E-mail yoon891023@snu.ac.kr; Tel. (+82) 2 880 8827; Fax (+82) 2 871 1993. E-mail yjseok@snu.ac.kr; Tel. (+82) 2 880 4414; Fax (+82) 2 871 1993. [†]These authors equally contributed to the work.

Introduction

Faecalibacterium prausnitzii, a Gram-positive bacterium extremely sensitive to oxygen, is one of the most abundant species among over 1,000 bacterial species constituting the intestinal microbiota of healthy human adults (Zoetendal *et al*., 2008; Arumugam *et al*., 2011). The abundance of this bacterium in the large intestine is negatively correlated with the severity of well-known chronic inflammatory diseases, such as inflammatory bowel disease and non-insulin-dependent (type II) diabetes (Sokol *et al*., 2008; Miquel *et al*., 2013; Cao *et al*., 2014; Gurung *et al*., 2020). Moreover, *F. prausnitzii* is known as a beneficial symbiont since it produces short-chain fatty acids, including butyrate, and anti-inflammatory substances exerting diverse effects on intestinal epithelial cells, such as enhancement of insulin sensitivity and improvement of gut motility (Flint *et al*., 2012; Tremaroli and Bäckhed, 2012; Breyner *et al*., 2017).

Despite the numerous studies conducted on the effect of *F. prausnitzii* metabolites on intestinal cells, studies that support such clinical importance are either limited to the confirmation of its growth on several carbon sources available in the gut (Duncan *et al*., 2002; Lopez-Siles *et al*., 2012; Miquel *et al*., 2014) or to its whole genome sequence analysis (El-Semman *et al*., 2014; Heinken *et al*., 2014; Fitzgerald *et al*., 2018). Although there has been an approach to reconstruct metabolic pathways of *F. prausnitzii* by examining its genome and predicting the transporters responsible for the import of specific carbon sources (Heinken *et al*., 2014), the bacteria still remains poorly characterized since substrate specificities of these presumed transporters or carbon source-dependent protein expressions of the relevant genes were not experimentally validated and functionally characterized.

Most bacteria rely on the phosphoenolpyruvate (PEP): carbohydrate phosphotransferase system (PTS) to efficiently import carbohydrates into cells by the concomitant transfer of phosphate from PEP to the incoming sugar (Deutscher *et al*., 2014). The PTS consists of two general

proteins shared for the transport of all PTS sugars, enzyme I (EI) and histidine-containing phosphocarrier protein (HPr), and several sugar-specific enzyme II (EII) complexes. The phosphoryl group is transferred from PEP to EI, HPr, EIIA, and finally to EIIB, which subsequently phosphorylates a PTS sugar during its translocation into the cell through EIIC. Thus, the phosphorylation states of the PTS components are modulated in response to the available carbon source (Deutscher *et al*., 2014). PTS components are also important as they play physiological roles by interacting with their cognate partners in a phosphorylation-dependent manner (Deutscher *et al*., 2006; Park *et al*., 2013; Kim *et al*., 2015; Park *et al*., 2016; Choe *et al*., 2017; Heo *et al*., 2019). Furthermore, in Gram-positive bacteria, it is known that the ATP-dependent phosphorylation of HPr on the Ser-46 residue by HPr kinase/phosphorylase (HPrK/P) (Mijakovic *et al*., 2002) is involved in physiological regulation, such as carbon catabolite repression, by binding to the global transcription regulator, catabolite control protein A (CcpA) (Singh *et al*., 2008). Therefore, a systematic functional analysis of the PTS components is crucial for understanding the basic physiology of most bacterial species.

F. prausnitzii A2-165 genome includes 16 genes encoding putative PTS components (Table 1) and one gene encoding HPrK/P (GenBank project accession PRJNA224116). In this study, we performed a systematic dissection of the PTS as the first step to understand how this species thrives in the human gut by utilizing specific carbohydrates and how PTS components regulate cell physiology based on the consumption of different nutrients in the gut.

Results

Transcription levels of putative PTS genes in F. prausnitzii *A2-165*

A recent study conducted on the identification of the metabolic capabilities of *F. prausnitzii* A2-165 suggested that several carbohydrates could be transported through the PTS (Heinken *et al*., 2014). However, the PTS genes have not been annotated clearly because the function of these proteins has not been validated. Therefore, by examining the recently updated reference genome of *F. prausnitzii* A2-165, we found 16 putative PTS genes among the 2,837 coding genes based on the gene annotations given by the NCBI database. The selected genes were compared to the genome of *F. prausnitzii* A2-165 in KEGG (NCBI PRJNA394904) for the verification of their annotations (Table 1). Thereafter, the protein sequences of these genes were aligned to the *Bacillus subtilis* 168 genome (NCBI PRJNA76), whose PTS components have been fully annotated. As a result, two EI homologues (encoded by GXM22_RS00575 and GXM22_RS01250), two HPr homologues (encoded by GXM22_RS01245 and GXM22_RS11900), and five putative sugar-specific enzyme II (EII) complexes consisting of 12 components were identified in the *F. prausnitzii* A2-165 genome (Fig. 1 and Table 1). An HPrK/P-encoding gene (GXM22_RS07750) is also present in the *F. prausnitzii* A2-165 genome, similar to that observed in other Gram-positive bacteria.

GXM22_RS01250 and GXM22_RS01245, encoding putative EI and HPr, respectively, are adjacent to each other, while GXM22_RS00575 and GXM22_RS11900 are located separately from other PTS genes in the chromosome. There are two contiguous PTS gene clusters, encoding two different mannose-family EIIs; GXM22_RS04175, RS04180, RS04185, and RS04190 encode EIID, EIIC, EIIB, and EIIA components, while GXM22_RS01340, RS01345, and RS01350 encode EIIB, EIIC, and EIID components, respectively. GXM22_RS01370, encoding a putative mannose-family EIIA component, is located near GXM22_RS01350. However, the genes encoding the *B. subtilis* glucose-specific EIIA homologue (GXM22_RS01420), fructose-specific EIIABC (GXM22_RS09805), and two glucose-family EIICBs (GXM22_RS00590 and RS14870) are scattered over the chromosome.

Since transcription of PTS genes is usually regulated in response to substrate availability (Plumbridge, 2001; Yoon *et al*., 2021), we measured the transcriptional level of the putative PTS genes by performing total RNA sequencing (RNA-seq) on the RNA samples extracted from *F. prausnitzii* cells grown on a PTS sugar (fructose, glucose), or *N*-acetylglucosamine (NAG), or on a putative non-PTS sugar (galactose) as the sole carbon source (Fig. 1). The transcription patterns of the general components demonstrated that the two contiguous genes, GXM22_RS01250 (putative *ptsI*) and GXM22_RS01245 (putative *ptsH*), were transcribed more in the presence of NAG and fructose than in the presence of glucose or galactose (Fig. 1). Additionally, through RT-PCR analysis, we found that GXM22_RS01250 and GXM22_RS01245 were co-transcribed as an operon (hereafter referred to as the *ptsHI* operon) in *F. prausnitzii* (Supporting Information Fig. S1), consistent with the findings in other bacteria (De Reuse and Danchin, 1988; Gonzy-Tréboul *et al*., 1989). However, the expression levels of other homologues of the general PTS components, GXM22_RS00575 (putative *ptsI*) and GXM22_RS11900 (putative *ptsH*), were not significantly influenced by the carbon source (Fig. 1).

Regarding the putative sugar-specific PTS components, the transcription of putative fructose-specific EIIABC (GXM22_RS09805, hereafter *fruA*) was 10-fold

Table 1. Putative PTS proteins of *F. prausnitzii* A2-165.

NCBI PRJNA224116		KEGG	*Bacillus subtilis* 168 BLASTp hit		Proposed annotation in this study
Locus	Annotation	Annotation	Protein	Identity (%)	
GXM22_RS00575	PEP-phosphotransferase	PTS system enzyme I (CG447_08375)[a]	PTS enzyme I (*ptsI*)	32	N.F.
GXM22_RS01250	PEP-phosphotransferase	PTS system enzyme I (CG447_07705)	PTS enzyme I (*ptsI*)	42	EI
GXM22_RS01245	HPr	Phosphocarrier protein HPr (CG447_07710)	HPr family phosphocarrier protein (*ptsH*)	40	HPr1
GXM22_RS11900	HPr	Phosphocarrier protein HPr (CG447_12060)	HPr family phosphocarrier protein (*ptsH*)	44	HPr2, HPrK/P substrate
GXM22_RS01420	PTS glucose transporter subunit IIA	PTS glucose transporter subunit IIA (CG447_07530)	beta-glucoside transporter subunit IIABC (*bglP*)	43	$EIIA^{NAG}$
GXM22_RS00590	PTS transporter subunit EIIC	*N*-acetylglucosamine PTS system EIICB component (CG447_08360)	*N*-acetylglucosamine-specific enzyme IICB component (*nagP*)	41	$EIICB^{NAG}$
GXM22_RS09805	PTS sugar transporter subunit IIA	Fructose PTS system EIIABC component (CG447_14155)	Fructose-specific enzyme IIABC component (*fruA*)	45	$EIIABC^{Fru}$
GXM22_RS14870	PTS transporter subunit EIIC	Maltose/glucose PTS system EIICB component (CG447_09070)	α-Glucoside-specific enzyme IICB component (*malP*)	30	Cryptic
GXM22_RS04190	PTS sugar transporter subunit IIA	Mannose PTS system EIIA component (CG447_04745)	Mannose/fructose/sorbose family IIA component	21[b]	N.F.
GXM22_RS04185	PTS sugar transporter subunit IIB	Mannose PTS system EIIB component (CG447_04750)	Mannose/fructose/sorbose family IIB component	28	N.F.
GXM22_RS04180	PTS sugar transporter subunit IIC	PTS sugar transporter subunit IIC (CG447_04755)	mannose/fructose/sorbose family IIC component	25	N.F.
GXM22_RS04175	PTS system mannose/ fructose/sorbose family transporter subunit IID	Fructoselysine/ glucoselysine PTS system EIID component (CG447_04760)	Mannose/fructose/sorbose family IID component	29[b]	N.F.
GXM22_RS01370	PTS sugar transporter subunit IIA	Mannose PTS system EIIA component (CG447_07580)	Mannose/fructose/sorbose family IIA component	22[b]	N.F.
GXM22_RS01340	PTS sugar transporter subunit IIB	Mannose PTS system EIIB component (CG447_07610)	Mannose/fructose/sorbose family IIB component	35	N.F.
GXM22_RS01345	PTS sugar transporter subunit IIC	Mannose PTS system EIIC component (CG447_07605)	Mannose/fructose/sorbose family IIC component	26	N.F.
GXM22_RS01350	PTS system mannose/ fructose/sorbose family transporter subunit IID	Fructoselysine/ glucoselysine PTS system EIID component (CG447_07600)	Mannose/fructose/sorbose family IID component	33	N.F.

N.F., non-functional.
[a]Locus tag identified on KEGG database (NCBI PRJNA394904).
[b]Sequence identity obtained through DELTA-BLAST due to no significant similarity using BLASTp.

higher in fructose-grown cells than in cells grown on other sugars. Unexpectedly, a confounding result was observed for the putative NAG-specific PTS transporter (GXM22_RS00590, hereafter *nagE*), as its transcription level was notably high in the presence of all sugars, yet significantly lower in NAG-grown cells compared to cells grown on glucose and galactose (Fig. 1). Furthermore, we found a putative gene cluster consisting of three NAG metabolism genes contiguous to *nagE*: GXM22_RS00595 encoding glucosamine-6-phosphate deaminase (*nagB*), GXM22_RS00600 encoding NAG deacetylase (*nagA*), and GXM22_RS00605 encoding *N*-acetyltransferase. Independently of the carbon source, these NAG metabolism genes were also highly expressed in all the tested media (Supporting Information Fig. S2). However, regardless of the carbon source, eight genes of two mannose-family PTS gene clusters and one gene encoding a glucose- or maltose-family EIICB protein (GXM22_RS14870) were

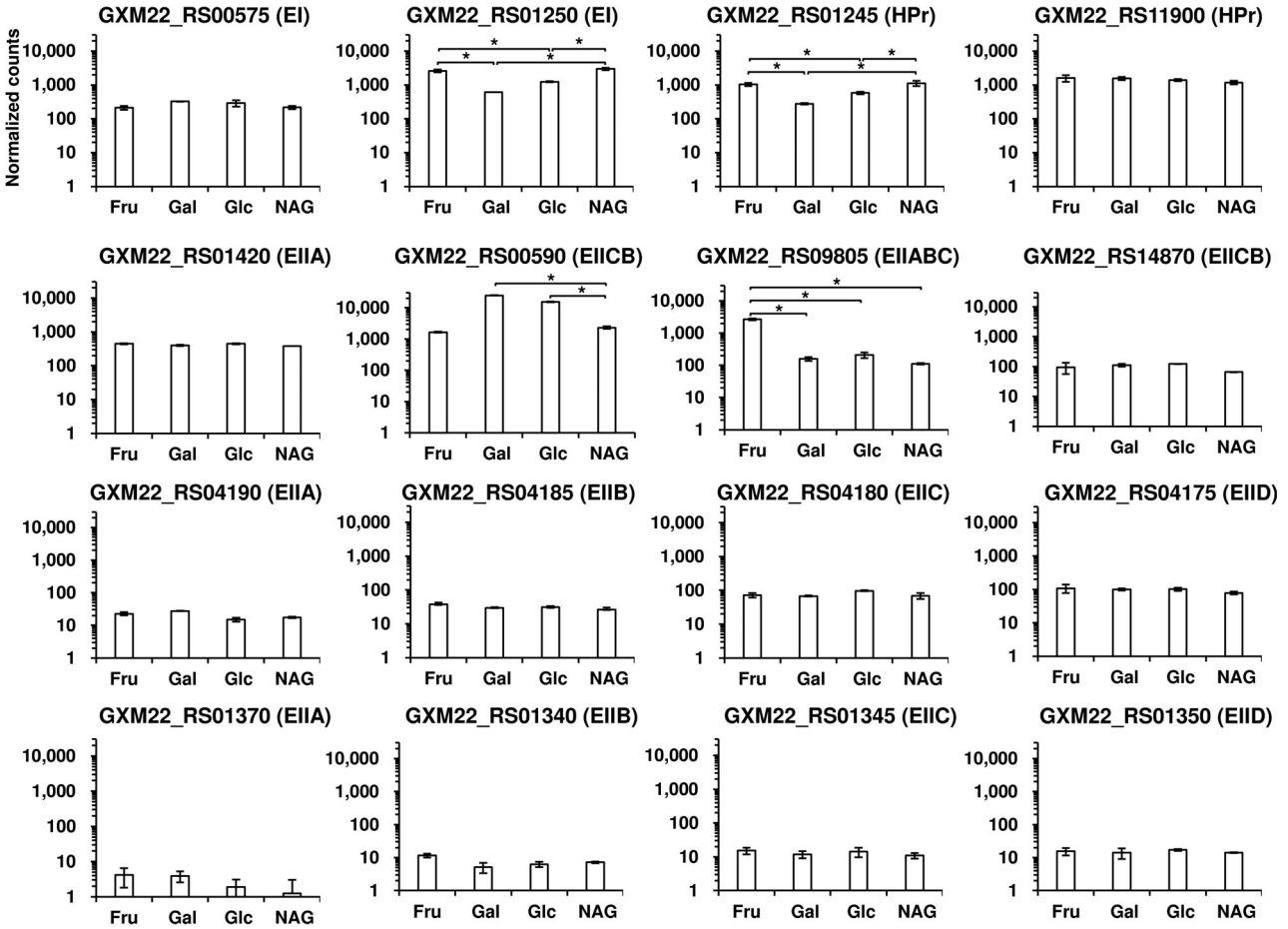

Fig. 1. Transcription levels of putative PTS genes in *F. prausnitzii* A2-165. Total RNA sequencing on cells grown on fructose (Fru), galactose (Gal), glucose (Glc), and *N*-acetylglucosamine (NAG), was performed to assess the transcription level of the PTS genes in *F. prausnitzii* A2-165. The comparison between the 16 putative PTS genes expressed in the presence of four sugars was conducted as described in the 'Experimental procedures' section. Error bars indicate the SD of data obtained from the analysis of two biological replicates. Y-axis refers to the normalized counts. *P*-values were adjusted by the Benjamini–Hochberg method, and *P*-values lower than 0.005 are indicated by asterisks.

expressed at very low levels, i.e., less than one-tenth of *fruA* (GXM22_ RS09805) transcription level in cells grown on fructose (Fig. 1).

Identification of functional EI and HPr

Direct insight into the function of a putative PTS gene may generally be obtained from its mutant phenotype (Reizer *et al*., 1995; Reizer *et al*., 1999; Hayes *et al*., 2017). However, as genetic manipulation is not feasible in *F. prausnitzii*, we conducted experiments to assess the phosphotransferase activity of EIs and HPrs and the sugar phosphorylation activity of EII components after overexpression and purification in *Escherichia coli*. To verify the activities of the general PTS components of *F. prausnitzii*, *in vitro* phosphorylation assays were performed using two EI homologues and HPr homologues. It is known that a phosphorylated HPr demonstrates higher mobility (phosphorylation-dependent electrophoretic mobility shift, PDEMS) than its unphosphorylated form in native-polyacrylamide gel electrophoresis (PAGE) (Gassner *et al*., 1977; Reizer *et al*., 1983), whereas EIIA usually shows decreased mobility in SDS-PAGE upon phosphorylation (Dörschug *et al*., 1984; Hogema *et al*., 1998; Lee *et al*., 2019). The native-PAGE data showed that neither of the two HPrs, herein referred to as HPr1 (GXM22_RS01245) and HPr2 (GXM22_RS11900), were phosphorylated by GXM22_RS00575-encoded EI, as no PDEMS was detected in the presence of PEP (Fig. 2A), indicating that the GXM22_RS00575 gene product was not functional, at least in terms of its phosphotransferase activity. The lack of phosphotransferase activity of the GXM22_RS00575 gene product was also confirmed by the absence of PDEMS of the EIIA encoded by GXM22_RS01420 in SDS-PAGE when incubated with either of the two HPrs and PEP (Supporting Information Fig. S3B, lanes 1, 2, 5, and 6). In contrast, the other EI homologue, encoded by GXM22_RS01250

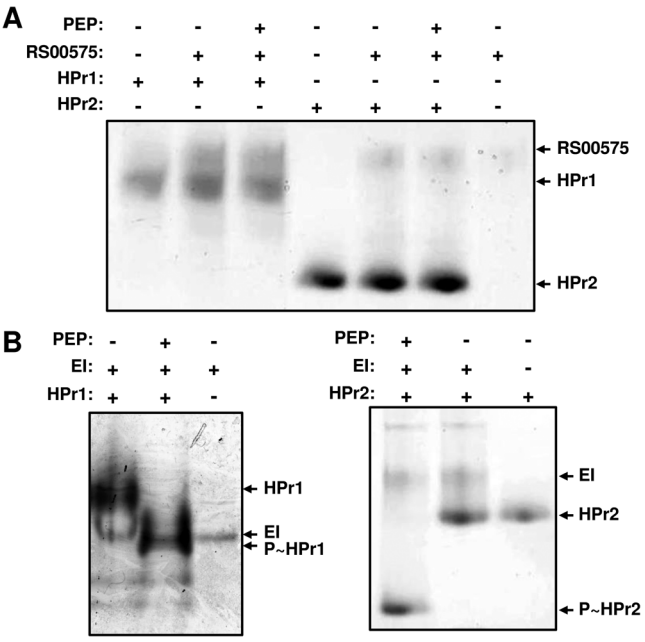

Fig. 2. Identification of EI participating in PEP-dependent phosphotransfer reaction. The proteins encoded by GXM22_RS00575 (A) or GXM22_RS01250 (B) (1 μg each) were purified and incubated with either HPr1 (3 μg) or HPr2 (2 μg) in buffer P (10 mM sodium phosphate, pH 8.0; 2 mM $MgCl_2$; 1 mM EDTA; 10 mM KCl; and 5 mM DTT) in the presence or absence of 1 mM PEP, to test the phosphotransferase activity of EI homologues. Each reaction mixture was analysed by conducting native-PAGE to measure the electrophoretic mobility shifts of HPrs as described in the 'Experimental procedures' section.

and co-transcribed with HPr1, exhibited phosphotransferase activity, as shown by the PDEMS of both HPr homologues in the presence of PEP (Fig. 2B). Despite the absence of phosphotransferase activity of EI (GXM22_RS00575), the amino acid sequences around the His residue responsible for the autophosphorylation by PEP (Alpert *et al*., 1985) were conserved in both EIs (Supporting Information Fig. S3A). Hence, we tried to observe the autophosphorylation of EI (GXM22_RS00575) by performing the identical phosphorylation assay with *E. coli* HPr (EcHPr) (Supporting Information Fig. S3B, lanes 3 and 4). As a result, we could observe the PDEMS of EIIA (GXM22_RS01420) in the reaction with EcHPr and PEP (Supporting Information Fig. S3B, lane 4). Therefore, we concluded that although both EI homologues could be autophosphorylated by PEP, only the GXM22_RS01250 gene product (hereafter referred to as *ptsI*, encoding EI) participated in the catalysis of PEP-dependent phosphoryl transfer reaction in *F. prausnitzii*.

It is known that HPrs of Gram-positive bacteria harbour another phosphorylation site at the Ser-46 residue, whose reaction is catalysed by ATP-dependent kinase HPrK/P (Deutscher *et al*., 2006). Interestingly, we found that two HPr homologues in *F. prausnitzii* A2-165 were distinguishable by the Ser-46 residue, which was only present in HPr2 (Fig. 3A). Therefore, we examined the HPrK/P-dependent phosphorylation of HPr homologues in the presence of ATP. As expected, HPr1 showed no band shift in native-PAGE upon incubation with HPrK/P and ATP (Fig. 3B). In contrast, HPr2 was phosphorylated by HPrK/P when ATP was added (Fig. 3C, lane 2). Interestingly, we found that the band shift of serine-phosphorylated HPr2 (HPr2[Ser-P]) could be distinguished from that of histidine-phosphorylated HPr2 (HPr2 [His-P]) due to the difference in mobility shift demonstrated on the native-PAGE gel (Fig. 3C, lanes 1 and 2). According to a previous study (Halbedel and Stülke, 2005), these two phosphorylation reactions are mutually exclusive, because phosphorylation at His-15 residue diminishes the affinity between HPrK/P and its protein substrate (Wang *et al*., 2000; Fieulaine *et al*., 2002; Deutscher *et al*., 2006). To confirm whether this was also true for *F. prausnitzii* HPr2, we conducted an *in vitro* phosphorylation assay in which phosphorylation reactions by HPrK/P and EI were performed concurrently (Fig. 3C, lane 3). Interestingly, incubation of HPr2 with HPrK/P and EI in the presence of PEP and ATP led to the formation of a doubly phosphorylated form, HPr2 (His-P/Ser-P), with a significant decrease in HPr2(His-P) in comparison to HPr2(Ser-P), thereby implying that under the employed experimental conditions, serine phosphorylation by HPrK/P constitutes the major phosphorylation event in HPr2 (Fig. 3C, lane 3).

After visualization of both the EI-dependent and HPrK/P-dependent phosphorylation reactions of the HPr homologues, we examined whether both HPr homologues could effectively transfer the phosphate group to the sugar-specific EIIAs. According to our analysis, three separately encoded EIIA proteins and one EIIA domain with seemingly different sugar specificities are encoded in the genome of *F. prausnitzii* A2-165 (Table 1). Among these, the EIIA encoded by gene GXM22_RS01420, predicted as an EIIA component specific for glucose or β-glucoside, was first analysed to determine its possible phosphorylation by HPrs. The phosphorylation state of EIIA was assessed by the PDEMS in SDS-PAGE, as described previously (Lee *et al*., 2019) and compared to that of two mutant forms mimicking phosphorylated and unphosphorylated EIIAs, EIIA(H93D) and EIIA(H93A), respectively. As expected due to the presence of the amino acid near the His-93 residue (Lee *et al*., 2019), the introduction of a negative charge at His-93 of EIIA by mutating it to Asp (H93D) caused slower migration of the protein (Fig. 4A, left panel), whereas mutation of His-93 to Ala (H93A) did not change its mobility in SDS-PAGE (Fig. 4A, right panel). To examine the HPr-mediated phosphotransfer from EI to EIIA, EIIA was mixed with EI and

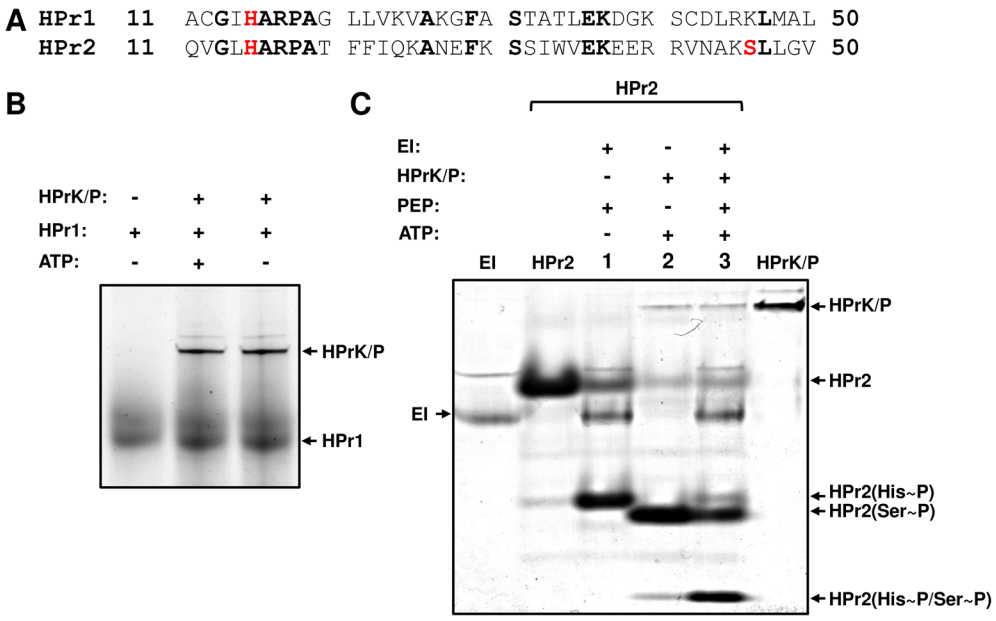

Fig. 3. HPr2 can be phosphorylated by both EI and HPrK/P.
A. Amino acid sequence alignment of HPr1 and HPr2. Identical amino acids are indicated in bold and the two phosphorylation sites of HPrs are indicated in red.
B. To test the phosphorylation of HPr1 by HPrK/P, HPr1 (3 μg) was incubated with HPrK/P (1 μg) in buffer P in the presence or absence of 4 mM ATP.
C. To test the phosphorylation of HPr2 by HPrK/P and EI, HPr2 (20 μg) was incubated with either HPrK/P or EI (3 μg each), or both (lane 1, 2, and 3, respectively), in buffer P in the presence or absence of 4 mM ATP and 4 mM PEP. Each reaction mixture was analysed by performing native-PAGE to measure the electrophoretic mobility shifts of HPrs as described in the 'Experimental procedures' section. [Color figure can be viewed at wileyonlinelibrary.com]

PEP in the presence of either of the two HPrs. As a result, HPr1 could phosphorylate 100% of EIIA, as shown by the phosphorylated band of EIIA identical to its phosphorylation mimic (Fig. 4A, left panel), whereas only 71% of EIIA was phosphorylated in the presence of HPr2 (Fig. 4A, right panel). To confirm this result, we performed an identical experiment using another EIIA protein, an EIIA domain of the putative fructose PTS (EIIABC^{Fru}) encoded by *fruA* (GXM22_RS09805). The EIIA^{Fru} domain was constructed by sub-cloning a DNA fragment encoding the first 146 amino acid residues of FruA. Since the wild-type EIIA^{Fru} domain did not show the PDEMS in SDS-PAGE, the Ser-110 residue was substituted with Asp to visualize the PDEMS as described previously (Lee *et al*., 2019). As expected, while the EIIA^{Fru}(S110D) domain could be fully phosphorylated by HPr1, only ~46% could be phosphorylated by HPr2 (Fig. 4B). Thus, we assume that HPr1 is the major HPr mediating the phosphoryl transfer from EI to EIIAs, whereas HPr2 may have distinct regulatory functions. Further observations of the phosphorelays between EI and EII proteins were therefore conducted using only HPr1.

Functional studies on sugar-specific PTS proteins

To observe the phosphorylation of PTS sugars by the cognate PTS proteins in *F. prausnitzii* and to identify the sugar specificities of the PTS membrane components, membrane proteins were extracted from *F. prausnitzii* cells grown on a single carbohydrate as the sole carbon source. Then an *in vitro* phosphotransferase assay was performed by mixing the membrane protein extracts with purified EI, HPr1, and EIIA in the presence of PEP and various carbohydrates. We assumed that, if the PTS-membrane proteins are expressed in cells grown on a PTS carbohydrate, the cognate EIIA will be dephosphorylated upon the addition of that sugar, since the phosphate group will be transferred from EIIA to the EII complex in the membrane, and finally to the incoming PTS sugar molecule. Therefore, the phosphorylation state of EIIA would represent the presence of functional carbohydrate-specific PTS proteins in the membrane protein extract. Since glucose was consumed by all *F. prausnitzii* strains (Duncan *et al*., 2002; Lopez-Siles *et al*., 2012), we anticipated that the glucose/glucoside-specific EIIA should be dephosphorylated in the presence of glucose and the membrane proteins extracted from glucose-grown *F. prausnitzii* cells. However, EIIA (GXM22_RS01420) was not dephosphorylated when glucose was added to the mixture of the membrane proteins extracted from glucose-grown cells in the presence of PEP, EI, and HPr1 (Fig. 5A). Interestingly, however, EIIA was dephosphorylated only when NAG was added to the

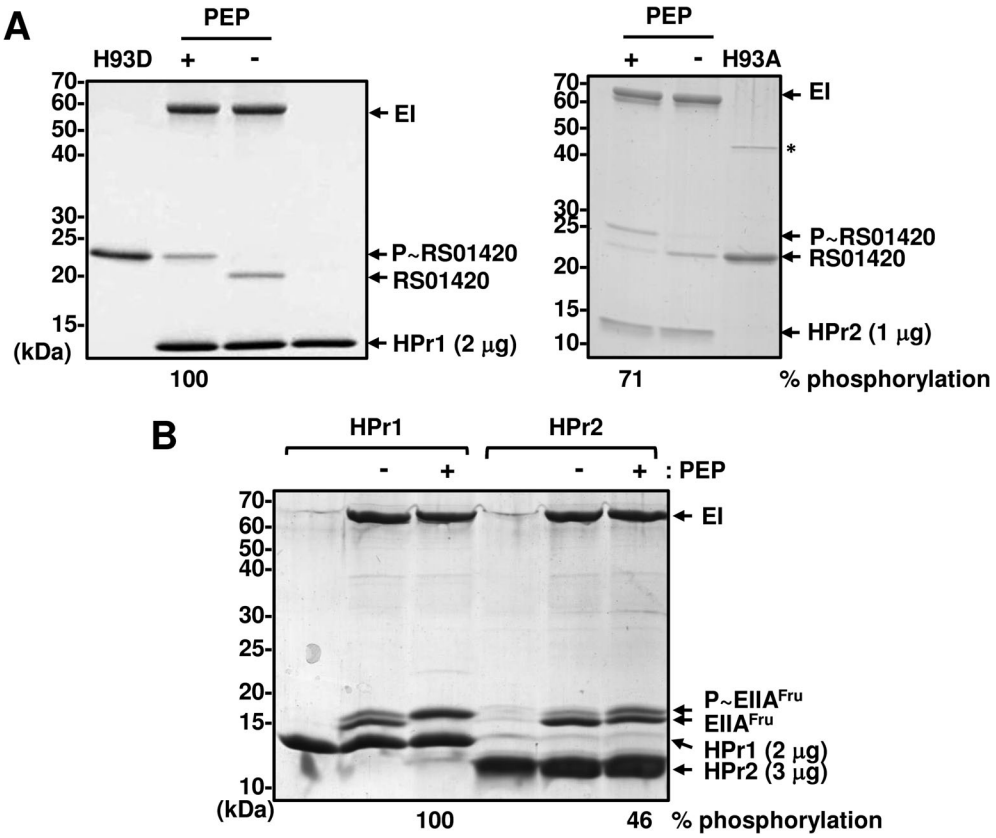

Fig. 4. HPr1 is the main phosphocarrier protein mediating the PEP-dependent phosphotransfer reaction. To test the phosphotransferase activity of HPrs, either HPr1 (left) or HPr2 (right) was incubated in buffer P with 1 μg of EIIA encoded by GXM22_RS01420 (A) or the EIIA domain of FruA in which Ser-110 was substituted with Asp (B) in the presence or absence of 1 mM PEP. After SDS-PAGE, the degree of EIIA phosphorylation was analysed using ImageJ software as described in 'Experimental procedures'. In (A), the phosphomimetic mutant (H93D) or the dephosphomimetic mutant (H93A) of the EIIA (2 μg each) was run as a control. An asterisk indicates a contaminant protein.

mixture containing membrane proteins extracted from NAG-grown cells (Fig. 5A). Based on this result, we annotated the EIIA encoded by GXM22_RS01420 as an EIIA specific for NAG ($EIIA^{NAG}$). To determine whether the functional NAG-specific PTS membrane protein was $EIICB^{NAG}$ encoded by GXM22_RS00590, annotated as *nagE* (Fig. 1 and Table 1), the putative $EIICB^{NAG}$ was overexpressed and purified in *E. coli*. Purified $EIICB^{NAG}$ was then mixed with EI, HPr1, and $EIIA^{NAG}$ in the presence of PEP and a carbohydrate such as glucose, NAG, fructose, mannose, or glycerol. As a result, $EIIA^{NAG}$ was dephosphorylated completely upon the addition of NAG and to some extent (~20%) upon the addition of glucose (Fig. 5B, lanes Glc and NAG). Thus, $EIICB^{NAG}$ seemed to have NAG as its main substrate and glucose with a much lower affinity. The results therefore show that $EIICB^{NAG}$ is expressed as a functional protein from *nagE* in *F. prausnitzii* A2-165 when the bacterium is consuming NAG.

Next, the import of fructose through the PTS was examined because fructose could also be efficiently utilized by all *F. prausnitzii* strains tested (Duncan *et al*., 2002; Lopez-Siles *et al*., 2012). The putative fructose-specific EIIABC is encoded by *fruA* (GXM22_RS09805) in *F. prausnitzii* A2-165 (Table 1). To confirm whether the fructose PTS components were specifically expressed in response to fructose as shown in Fig. 1, EI, HPr1, $EIIA^{Fru}$(S110D), and PEP were mixed with fructose and the membrane proteins extracted from cells grown on various carbohydrates including mannose, galactose, NAG, glucose, and fructose. This result showed that $EIIA^{Fru}$(S110D) could be dephosphorylated by fructose only when the membrane proteins extracted from the cells grown on fructose were added (Fig. 6A). Next, to observe the sugar specificity of FruA, the membrane protein extract of fructose-grown cells was mixed with the general PTS components, $EIIA^{Fru}$(S110D), PEP, and various carbohydrates. As a result, $EIIA^{Fru}$(S110D) could be dephosphorylated only in the presence of fructose but not in the presence of galactose, maltose, NAG, glucose, mannose, and *N*-acetylgalactosamine (GalNAc) (Fig. 6B). Therefore, we conclude that FruA is expressed specifically

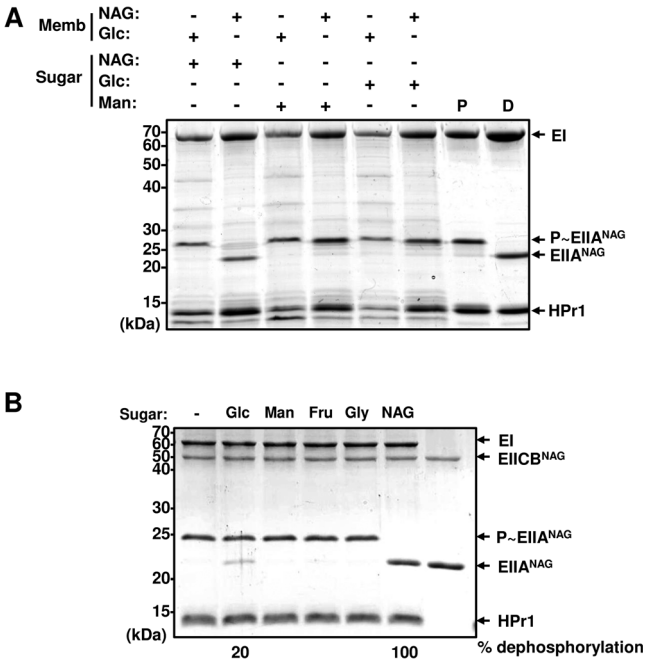

Fig. 5. Detection of the sugar phosphorylation activity of *N*-acetylglucosamine-specific enzyme II. *In vitro* phosphotransferase assays were performed to measure the sugar phosphorylation activity of the membrane protein extracts (A) and purified $EIICB^{NAG}$ (B). Membrane protein extracts (Memb) were prepared from *F. prausnitzii* cells grown on glucose or NAG as indicated. The membrane protein extract (4 μg) or purified $EIICB^{NAG}$ (0.5 μg) was incubated with three soluble PTS proteins (1 μg of EI, 3 μg of HPr1, and 1 μg of $EIIA^{NAG}$) in buffer P in the presence of 0.1 mM PEP and the indicated recipient sugars (2 mM). Reaction mixtures of EI, HPr1, and $EIIA^{NAG}$ in the presence (lane P) or absence (lane D) of 0.1 mM PEP without the addition of any membrane fractions and recipient sugars served as a control. NAG, *N*-acetylglucosamine; Glc, glucose; Man, mannose; Fru, fructose; Gly, glycerol.

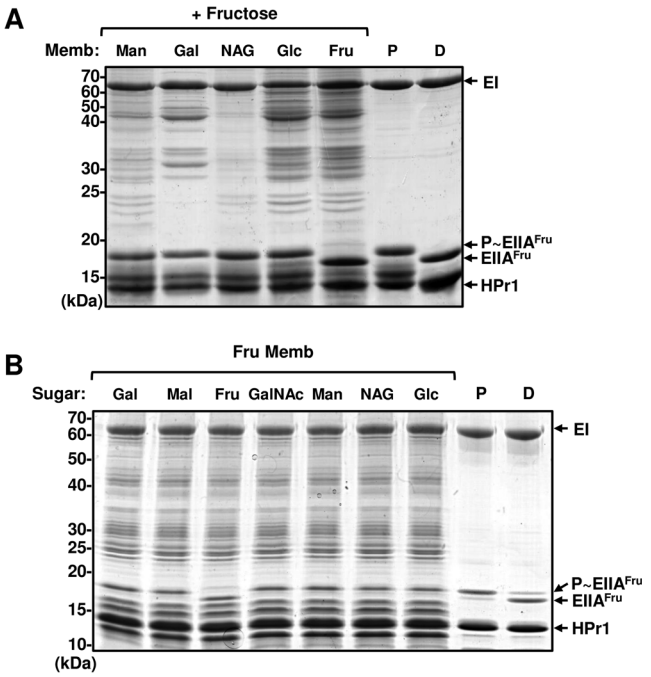

Fig. 6. Fructose-specific enzyme II is expressed exclusively in the presence of fructose. *In vitro* phosphotransferase assays were performed to investigate the expression condition and substrate specificity of $EIIABC^{Fru}$.

A. Membrane protein extracts (Memb) were prepared from *F. prausnitzii* cells grown on the indicated sugars and each extract (4 μg) was incubated with EI (2 μg), HPr1 (3 μg), and $EIIA^{Fru}$(S110D) (2 μg) in buffer P in the presence of 0.1 mM PEP and 2 mM of fructose.

B. The membrane protein extract prepared from *F. prausnitzii* cells grown on fructose was incubated with EI (2 μg), HPr1 (2 μg), and $EIIA^{Fru}$(S110D) (1 μg) in buffer P in the presence of 0.1 mM PEP and 2 mM of the indicated sugar. Reaction mixtures were analysed by conducting SDS-PAGE to measure the electrophoretic mobility shifts of $EIIA^{Fru}$. The reaction mixture of EI, HPr1, and $EIIA^{Fru}$(S110D) in the presence (lane P) or absence (lane D) of 0.1 mM PEP without the addition of any membrane fractions or sugars served as a control. Gal, galactose; Mal, maltose; GalNAc, *N*-acetylgalactosamine.

in the presence of fructose, and the fructose-PTS only participates in the transportation of fructose in *F. prausnitzii* A2-165.

Non-functional or cryptic PTS components

It has been previously reported that *F. prausnitzii* A2-165 could not metabolize mannose: the mannose-catabolism gene cluster exists only in some strains of *F. prausnitzii*, other than A2-165 (Martín *et al*., 2017; Fitzgerald *et al*., 2018). Because the transcription levels of the eight genes encoding two mannose-family EIIs were very low regardless of the carbon sources (Table 1 and Fig. 1), we wondered whether these gene products were functional. We, therefore, tested their functionality by conducting *in vitro* phosphotransferase assay to observe the PDEMS in native- or SDS-PAGE in the presence of PEP, as shown in Fig. 4. Interestingly, GXM22_RS04190 and GXM22_RS01370 encoding EIIAs have highly similar sequences (72%) (Supporting Information Fig. S4A). The two mannose-family EIIAs did not demonstrate any PDEMS on native-PAGE gels in the presence of PEP and general PTS components (Supporting Information Fig. S4B and E). In addition, when the identical sets of samples were subjected to analysis by SDS-PAGE, we could not observe a phosphorylation-dependent upshift of the two putative mannose-specific EIIAs (Supporting Information Fig. S4C and F). Hence, in a final effort to visualize phosphorylation at His-9, if it ever occurs, we substituted Ser-10 and Ala-16 of EIIA (GXM22_RS04190) with aspartate (SA → D) to induce PDEMS in SDS-PAGE (Lee *et al*., 2019). Despite the introduction of negative charges nearby the expected phosphorylation site of His-9 (Supporting Information Fig. S4A), the EIIA encoded by GXM22_RS04190 did not demonstrate PDEMS in the presence of PEP,

whereas $EIIA^{NAG}$ did (Supporting Information Fig. S4D, lanes 2 and 4). Hence, we conclude that both GXM22_RS04190 and GXM22_RS01370 are non-functional and so are the contiguous EIIBC or D (GXM22_RS04185 to RS04175 and GXM22_RS01340 to RS01350).

Regarding the putative glucose/maltose-specific EIIBC encoded by GXM22_RS14870, we confirmed by RNA-seq that the gene was scarcely expressed in glucose medium (Table 1 and Fig. 1). Since we have confirmed that the membrane proteins extracted from cells grown on a PTS sugar contain the cognate PTS components, as seen in fructose- or NAG-grown cells (Figs. 5A and 6A), we assumed that the EIIBC encoded by GXM22_RS14870 would be present in the membrane fraction extracted from glucose- or maltose-grown cells. To verify this assumption, we mixed purified EI, HPr1, and $EIIA^{NAG}$, which is the only functional form of the three separately encoded EIIAs, with membrane proteins extracted from glucose- or maltose-grown cells in addition to PEP, to observe whether any dephosphorylation of $EIIA^{NAG}$ occurs by the addition of glucose or maltose (Supporting Information Fig. S5). Unexpectedly, however, we could not see any dephosphorylation of $EIIA^{NAG}$ in either of the two membrane protein extracts in the presence of glucose, maltose, GalNAc, NAG, or mannose (Supporting Information Fig. S5A and B). Furthermore, EIIBC (GXM22_RS14870) did not have any activity towards other glucose-containing disaccharides (Supporting Information Fig. S5C). Finally, since *F. prausnitzii* is known to consume glucosamine (GlcN) (Duncan *et al*., 2002; Lopez-Siles *et al*., 2012; Miquel *et al*., 2014), we tried to test the possibility of GXM22_RS14870 being the PTS transporter for GlcN. Membrane protein extracts were prepared from the cells grown on GlcN and an identical phosphotransferase assay was performed (Supporting Information Fig. S5D). As a result, we could not observe dephosphorylation of $EIIA^{NAG}$ by the addition of GlcN to the extent greater than the addition of any other sugars or no sugar. Therefore, we conclude that EIIBC (GXM22_RS14870) is a cryptic PTS protein.

Discussion

The phosphorylation state of PTS proteins reflects the availability of sugars and the consequent physiological state of the cell to the activity of transport proteins, metabolic enzymes, and transcriptional regulators. Such a complex yet plastic regulation provides a significant evolutionary advantage to bacteria (Stülke and Hillen, 1998). On a larger scope, studying PTS proteins is important because the cellular intake of carbohydrates and the subsequent synthesis and secretion of microbial metabolites by such abundant bacteria as *F. prausnitzii* may shape the whole nutrient profile in the large intestine, with a substantial impact exerted on the overall gut microbiota and host cells (Macfarlane *et al*., 1998). This study highlights the physiological characteristics of *F. prausnitzii* using biochemical *in vitro* approaches. We have provided an overall model of the PTS in *F. prausnitzii* A2-165 (Fig. 7) by reannotating the presumed PTS genes of the bacterium through protein sequence alignment and performing *in vitro* phosphotransferase assays using the membranous protein extracts from *F. prausnitzii* cells grown on diverse carbohydrates and the purified PTS proteins.

This study has revealed several unique features of the PTS in *F. prausnitzii* A2-165, which possesses two copies of each of the general components; the results show that the functionality of the general PTS components is different between the two homologues.

While only the EI encoded by gene GXM22_RS01250 showed phosphotransferase activity, both HPrs were functional yet displayed a difference in performance. We speculate that HPr1 mainly participates in transferring the PEP-derived phosphate group from EI to EIIAs, while HPr2 may be involved in regulatory roles owing to its phosphorylation at Ser-46 (Fig. 2C) (Poncet *et al*., 2009), rather than in the phosphotransferase reactions. The Ser-46 phosphorylation of HPr in Gram-positive bacteria has been known to be involved in numerous physiological regulations, such as amino acid metabolism and carbon catabolite repression, as a cofactor for CcpA (Stülke and Hillen, 1998). A previous study on the glycerol kinase of *Enterococcus faecalis* showed that a doubly phosphorylated form of HPr could lead to the phosphorylation of glycerol kinase more efficiently than His-15 phosphorylated HPr (Reizer *et al*., 1993), postulating that a doubly phosphorylated HPr2 might also function as a phosphoryl donor protein in *F. prausnitzii* to its interacting partners. Hence, the roles of HPr2 in *F. prausnitzii* remain to be investigated.

In addition to EI and HPr, we assessed the functionality of all EII complexes; while FruA ($EIIABC^{Fru}$) and NagE ($EIICB^{NAG}$) were expressed as functional forms, the remaining three EII complexes appeared to be non-functional in *F. prausnitzii* A2-165. We found that the gene coding for the putative 1-phosphofructokinase (*fruK*), which converts fructose 1-phosphate into fructose 1, 6-bisphosphate, is adjacent to the gene encoding $EIIABC^{Fru}$. Additionally, we found that a transcriptional regulator with ~40% protein sequence identity with the *B. subtilis* 168 fructose repressor FruR is also encoded adjacent to *fruK*. The presence of the fructose-specific PTS and fructose metabolic enzymes in *F. prausnitzii* may explain why the supplementation of fructo-oligosaccharides or inulin in diets has led to increased *F. prausnitzii* abundance in patients with obesity and

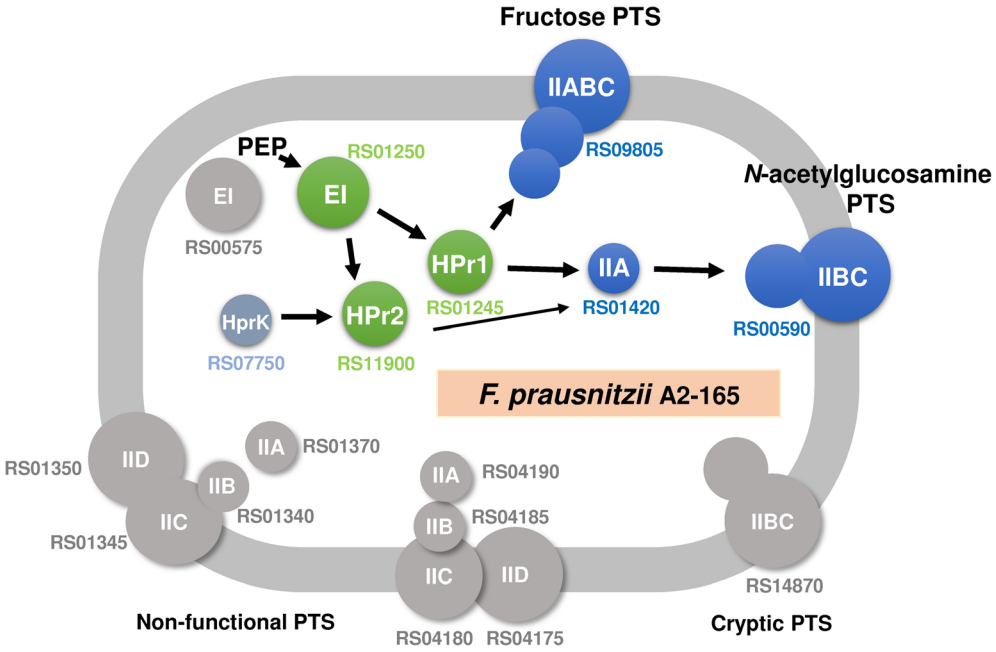

Fig. 7. Overview of the PTS in *F. prausnitzii* A2-165. Among the 16 PTS components identified through genomic analysis, EI and HPr1 actively participated in the phosphotransfer reaction to import NAG and fructose translocated through their cognate PTS membrane components. HPr2, which can be phosphorylated by HPrK/P, appears to play regulatory roles different from those played by HPr1. One of the EI homologues and other sugar-specific EIIBC complexes are likely to be non-functional or cryptic. [Color figure can be viewed at wileyonlinelibrary.com]

irritable bowel syndrome (Clavel *et al*., 2005; Dewulf *et al*., 2013; Hustoft *et al*., 2017), implying the significance of FruA for the prevalence of *F. prausnitzii* in the gut over other species. It has also been reported that extra dietary fructose can nourish gut microbes that produce short-chain fatty acids (Jang *et al*., 2018). Therefore, it is also likely that the presence of *F. prausnitzii* possessing FruA in the gut may confer a major benefit to the host health.

Since the outer layer of vertebrate mucin consists of various complex carbohydrates and glycans that are mostly rich in the amino sugar NAG (Dekker *et al*., 1991; Wlodarska *et al*., 2017), efficient transportation of NAG into the cell through the PTS would be advantageous to bacteria residing in the gut. Similar to the fructose-metabolizing gene cluster, genes encoding *N*-acetylglucosamine 6-phosphate deacetylase and glucosamine 6-phosphate deaminase required to utilize this amino sugar (Supporting Information Fig. S2) are adjacent to *nagE*. As the gene encoding NAG-specific PTS (PTS^{NAG}) has been reported as one of the most abundant transporter genes encoded in the commensal Clostridiales order (Wlodarska *et al*., 2017), it can be assumed that *F. prausnitzii*, which belongs to it, actively metabolizes NAG through PTS in the gut.

Despite the presence of putative genes encoding membrane PTS proteins specific for glucose, mannose, and maltose (Table 1), the transcription levels of these genes could only barely be detected and their functionalities were not observed through our methods (Supporting Information Figs. S4 and S5). Interestingly, although glucose is utilized by most strains of *F. prausnitzii* (Duncan *et al*., 2002; Heinken *et al*., 2014), it appears to be transported by mechanisms other than the PTS in *F. prausnitzii* A2-165 (Supporting Information Fig. S5A and C). Since glucose from diet is readily absorbed by the host epithelial cells as well as other bacteria in the small intestine (Utzschneider *et al*., 2016; Woting and Blaut, 2016), it is a relatively scarce nutrient in the distal colon, where *F. prausnitzii* resides (Duncan *et al*., 2009; Lopez-Siles *et al*., 2016). Intriguingly, *Bifidobacterium bifidum* MB245 and *Bifidobacterium lactis* DSM10140, the common anaerobes also residing in large intestines of animals, only harbour the fructose-specific PTS, consuming glucose only through facilitated diffusion (Barabote and Saier, 2005; Briczinski *et al*., 2008). As one of the most common constituents of dietary probiotics, they successfully colonize the large intestine even after belated introduction (Bartosch *et al*., 2005), implying that possession of the fructose and NAG PTS rather than the glucose PTS may confer some selective advantage for the bacteria to compete against other species in the gut (Briczinski *et al*., 2008).

We believe that the investigation on the PTS in *F. prausnitzii* may contribute to understanding how this commensal bacterium can colonize and thrive as a

dominant species in the human gut. In the future, a detailed characterization of the physiological responses of *F. prausnitzii* with respect to the available nutrients will help us to identify the conditions necessary for its proliferation in the gut, offering further clues on the same for several beneficial Firmicutes.

Experimental procedures

Bacterial strains, plasmids, and culture conditions

The bacterial strains and plasmids used in this study are listed in the Supporting Information Table S1 and S2. The *F. prausnitzii* strain A2-165 (DSM17677) used in this study was purchased from DSMZ (Braunschweig, Germany) and was cultured under anaerobic conditions at 37°C in yeast extract-casein hydrolysate-fatty acids (YCFA) medium supplemented with the indicated filter-sterilized carbon sources (final concentration: 0.5% w/v) (Duncan *et al*., 2003). The YCFA medium contained (per 200 ml) 2 g of casitone, 0.5 g of yeast extract, 1 g of glucose, 9 mg of $MgSO_4{\cdot}7H_2O$, 18 mg of $CaCl_2{\cdot}2H_2O$, 90 mg of K_2HPO_4, 90 mg of KH_2PO_4, 0.18 g of NaCl, 0.2 mg of resazurin, 0.8 g of $NaHCO_3$, 0.2 g of L-cysteine-HCl, and 2 mg of hemin, supplemented with a filter-sterilized vitamin solution consisting of 2 μg of biotin, 2 μg of folic acid, 10 μg of pyridoxine-HCl, 5 μg of thiamine-$HCl{\cdot}2H_2O$, 5 μg of D-Ca-pantothenate, 5 μg of riboflavin, 5 μg of nicotinic acid, 0.1 μg of vitamin B12, 5 μg of 4-aminobenzoic acid, and 5 μg of lipoid acid. Short-chain fatty acids were added to reach the following final concentrations (v/v): 0.19% acetic acid, 0.07% propionic acid, 0.009% isobutyric acid, 0.01% *n*-valeric acid, and 0.01% isovaleric acid. For overexpression of recombinant proteins, *E. coli* strains were cultured in Luria Bertani (LB) medium consisting of 1% tryptone, 0.5% NaCl, and 0.5% yeast extract at 37°C. The following were added if necessary: 50 μg ml^{-1} kanamycin for *E. coli*; 100 μg ml^{-1} ampicillin for *E. coli*; 0.5 μg ml^{-1} ciprofloxacin for *F. prausnitzii*; 1 mM isopropyl-b-D-1-thiogalactopyranoside for overexpression of recombinant proteins in *E. coli*.

The genomic DNA of *F. prausnitzii* A2-165 was extracted using the QIAamp® DNA Mini Kit (Qiagen, Germantown, MD) according to the manufacturer's instructions and used as the template for the amplification of PTS genes. The PCR products were digested with BamHI and SalI, or NdeI and XhoI (New England Biolabs, Beverley, MA) and inserted into the corresponding site of the plasmid pETDuet-1. Amino acid substitution mutants of EIIAs and HPr1 were generated by site-directed mutagenesis PCR using appropriate primer pairs (Supporting Information Table S2). All plasmid constructs were confirmed by performing PCR and sequencing.

Purification of proteins

Proteins were expressed from pETDuet-1 vectors in *E. coli* ER2566 Δ*pts* (Park *et al*., 2013) (Supporting Information Table S1). Harvested cells were resuspended in buffer A (20 mM sodium phosphate, pH 8.0; 5 mM β-mercaptoethanol; and 5% glycerol) containing 200 mM NaCl and then disrupted by ultrasonication. The cell lysates were centrifuged at 100 000 × *g* at 4°C for 1 h to remove cell debris. Untagged proteins were purified using the MonoQ™ 10/100 GL and the HiLoad 16/60 Superdex 200 prep grade columns (GE Healthcare Life Science, Marlborough, MA). After removal of cell debris, the lysate was applied to a Mono Q™ 10/100 GL (GE Healthcare Life Science) column equilibrated with buffer A, containing 50 mM NaCl. The protein fraction was eluted using buffer A with 0.05–1 M NaCl gradient at a flow rate of 2 ml min^{-1}. The fractions containing the desired proteins were concentrated using Amicon Ultracel-3K centrifugal filters (Merck Millipore, Burlington, MA) and were subjected to chromatography using the HiLoad 16/60 Superdex 200 prep grade column (GE Healthcare Life Science) equilibrated with buffer A containing 200 mM NaCl (buffer B) to achieve higher purity.

His-tagged proteins were purified by performing immobilized metal affinity chromatography using a TALON metal affinity resin (Takara Bio, Otsu, Japan) according to the manufacturer's instructions. Resin-bound proteins were subjected to washing steps three times using buffer B containing 10 mM imidazole and eluted with 200 mM imidazole. To remove imidazole and increase purity, proteins were subjected to chromatography using the HiLoad 16/600 Superdex 200 prep grade column (GE Healthcare Life Science) equilibrated with buffer B.

His-tagged $EIICB^{NAG}$ was purified from the *E. coli* cell membrane after solubilization with 1% n-dodecyl-β-D-maltopyranoside (DDM). After removal of cell debris from the lysate, the membrane was centrifuged at 100 000 × *g* at 4°C for 1 h to obtain the membrane in a pellet form. The pellet was resuspended in buffer B containing 1% DDM and centrifuged again at 100 ,000 × *g* at 4°C for 30 min. His-$EIICB^{NAG}$ was purified using a TALON metal affinity resin (Takara Bio) as described above, except for the addition of 0.1% DDM in wash and elution buffer. The eluted proteins were further chromatographed on the HiLoad 16/600 Superdex 200 prep grade column (GE Healthcare Life Science) equilibrated with buffer B containing 0.05% DDM. Purified proteins were concentrated using Amicon Ultracel-3K centrifugal filters (Merck Millipore), and total protein concentration was determined by performing the Bradford protein assay using bovine serum albumin as the standard.

Extraction of the membrane proteins from F. prausnitzii

F. prausnitzii A2-165 cells grown on the indicated sugars were harvested after 36 h, subjected to washing steps with buffer C (20 mM Tris–HCl, pH 8; 150 mM NaCl; 1 mM phenylmethylsulfonyl fluoride; 10 mM $MgCl_2$; 10% glycerol; and 5 mM β-mercaptoethanol) and centrifuged at 9300 × *g* at 4°C for 15 min. The cell pellet obtained after centrifugation was resuspended in buffer C and frozen at −80°C with the addition of protease inhibitor (Sigma-Aldrich, Waltham, MA) to lyse the cells. The cells were disrupted by ultrasonication and then centrifuged at 9300 × *g* at 4°C for 15 min to remove cell debris. The cell lysates were further centrifuged at 100 000 × *g* at 4°C for 1 h, and the resulting pellets were resuspended in buffer B containing 1% DDM. The solubilized membrane fraction was centrifuged at 10 000 × *g* at 4°C for 20 min to remove any remaining debris.

In vitro *phosphorylation assay*

All phosphorylation assays were performed using buffer P (10 mM sodium phosphate, pH 8.0; 2 mM $MgCl_2$; 1 mM EDTA; 10 mM KCl; and 5 mM DTT) and the following purified proteins, if not indicated otherwise: 1 μg of EI homologues, 3 μg of HPr1, 2 μg of HPr2, 1 μg of HPrK/P, and 1 μg of EIIAs. The reaction mixtures, if not indicated otherwise, were incubated for 10 min at 37°C in the presence of 1 mM PEP, 1 mM pyruvate, or 4 mM ATP. Each reaction mixture was subjected to analysis on a 4%–20% gradient or 16% polyacrylamide gel for SDS-PAGE and 10% for native-PAGE (acrylamide/bisacrylamide ratio of 37.5:1) (KOMA Biotech, Seoul, South Korea) in Tris-Glycine (25 mM Tris, 192 mM Glycine) buffer supplemented with or without 0.1% SDS followed by Coomassie Brilliant Blue R staining. PTS-dependent sugar phosphorylation assays were conducted in an identical manner using three soluble PTS proteins (1 μg of EI, 3 μg of HPr1, and 2 μg of EIIAs), 0.5 μg of $EIICB^{NAG}$, and 4 μg of total membrane protein extracts in combinations as indicated. The reaction mixtures were incubated for 10 min at 37°C in the presence of 0.1 mM PEP and 2 mM of the indicated carbohydrates. The protein band intensities were quantified using the ImageJ software (NIH Image, National Institutes of Health, Bethesda, MD; available online at http://rsbweb.nih.gov/ij/).

RNA extraction from the F. prausnitzii *cells grown on a single carbohydrate*

F. prausnitzii A2-165 cells cultured overnight were diluted 100-fold in 10 ml of fresh YCFA medium supplemented with the indicated filter-sterilized carbon sources in 0.5% (w/v) final concentration and incubated at 37°C until OD_{600} reached 0.4 for galactose and glucose and 0.2 for fructose and NAG. After fixing the cells with the same volume of 100% methanol for 1 h at −20°C, total RNA was extracted using the phenol-chloroform extraction method (Kim *et al*., 2020); the isolated RNAs were further purified using the TaKaRa MiniBEST Universal RNA Extraction Kit (Takara Bio) according to the manufacturer's instructions. Two biological replicates were performed for each sample.

RNA sample preparation and sequencing

One microgram of total RNA was processed to deplete the ribosomal RNA using NEBNext rRNA Depletion Kit (Bacteria) (#E7850, NEB). Sequencing libraries for RNA-seq were constructed using the NEBNext Ultra II RNA Library Prep Kit for Illumina (#E7770, NEB) following the manufacturer's instructions. Sequencing was performed on an NextSeq 500 instrument (Illumina) following the manufacturer's protocol and generated 76 bp paired-end reads for each sample.

RNA-seq data processing and analysis

The sequencing adapter removal and quality-based trimming of raw data was performed using Trimmomatic v. 0.36 (Bolger *et al*., 2014) with TruSeq adapter sequences. Cleaned reads were mapped to the reference genome of *F. prausnitzii* A2-165, which is available in GenBank accession number PRJNA224116 (https://www.ncbi.nlm.nih.gov/nuccore/NZ_CP048437.1) using hisat2 (Kim *et al*., 2019) with '--no-spliced-alignment' parameter. For counting reads, which mapped to each coding DNA sequence, featureCounts (Liao *et al*., 2014) was used. Retrieved counts were normalized and analysed to identify differentially expressed genes with DESeq2 (Love *et al*., 2014).

Acknowledgements

The authors thank Dr. Kyoo Heo, Dr. Ji-Hee Yoon, and Hye-Young Lee (Seoul National University) for the helpful discussions. This work was supported by National Research Foundation Grants NRF-2018R1A5A1025077 and NRF-2019R1A2C2004143 funded by the Ministry of Science, South Korea.

Data availability

All gene expression files are available from the Gene Expression Omnibus database under the accession number GSE168352. The datasets used and/or analysed

during the current study are available from the corresponding authors on reasonable request.

References

Alpert, C.A., Frank, R., Stüber, K., Deutscher, J., and Hengstenberg, W. (1985) Phosphoenolpyruvate-dependent protein kinase enzyme I of *Streptococcus faecalis*: purification and properties of the enzyme and characterization of its active center. *Biochemistry* **24**: 959–964.

Arumugam, M., Raes, J., Pelletier, E., Le Paslier, D., Yamada, T., Mende, D.R., *et al*. (2011) Enterotypes of the human gut microbiome. *Nature* **473**: 174–180.

Barabote, R.D., and Saier, M.H. (2005) Comparative genomic analyses of the bacterial phosphotransferase system. *Microbiol Mol Biol Rev* **69**: 608–634.

Bartosch, S., Woodmansey, E.J., Paterson, J.C., McMurdo, M.E., and Macfarlane, G.T. (2005) Microbiological effects of consuming a synbiotic containing *Bifidobacterium bifidum*, *Bifidobacterium lactis*, and oligofructose in elderly persons, determined by real-time polymerase chain reaction and counting of viable bacteria. *Clin Infect Dis* **40**: 28–37.

Bolger, A.M., Lohse, M., and Usadel, B. (2014) Trimmomatic: a flexible trimmer for Illumina sequence data. *Bioinformatics* **30**: 2114–2120.

Breyner, N.M., Michon, C., de Sousa, C.S., Vilas Boas, P.B., Chain, F., Azevedo, V.A., *et al*. (2017) Microbial anti-inflammatory molecule (MAM) from *Faecalibacterium prausnitzii* shows a protective effect on DNBS and DSS-induced colitis model in mice through inhibition of NF-κB pathway. *Front Microbiol* **8**: 114.

Briczinski, E.P., Phillips, A.T., and Roberts, R.F. (2008) Transport of glucose by *Bifidobacterium animalis* subsp. *lactis* occurs via facilitated diffusion. *Appl Environ Microbiol* **74**: 6941–6948.

Cao, Y., Shen, J., and Ran, Z.H. (2014) Association between *Faecalibacterium prausnitzii* reduction and inflammatory bowel disease: a meta-analysis and systematic review of the literature. *Gastroenterol Res Pract* **2014**: 872725.

Choe, M., Park, Y.H., Lee, C.R., Kim, Y.R., and Seok, Y.J. (2017) The general PTS component HPr determines the preference for glucose over mannitol. *Sci Rep* **7**: 43431.

Clavel, T., Fallani, M., Lepage, P., Levenez, F., Mathey, J., Rochet, V., *et al*. (2005) Isoflavones and functional foods alter the dominant intestinal microbiota in postmenopausal women. *J Nutr* **135**: 2786–2792.

De Reuse, H., and Danchin, A. (1988) The *ptsH*, *ptsI*, and *crr* genes of the *Escherichia coli* phosphoenolpyruvate-dependent phosphotransferase system: a complex operon with several modes of transcription. *J Bacteriol* **170**: 3827–3837.

Dekker, J., Aelmans, P.H., and Strous, G.J. (1991) The oligomeric structure of rat and human gastric mucins. *Biochem J* **277**: 423–427.

Deutscher, J., Francke, C., and Postma, P.W. (2006) How phosphotransferase system-related protein phosphorylation regulates carbohydrate metabolism in bacteria. *Microbiol Mol Biol Rev* **70**: 939–1031.

Deutscher, J., Aké, F.M., Derkaoui, M., Zébré, A.C., Cao, T. N., Bouraoui, H., *et al*. (2014) The bacterial phosphoenolpyruvate:carbohydrate phosphotransferase system: regulation by protein phosphorylation and phosphorylation-dependent protein-protein interactions. *Microbiol Mol Biol Rev* **78**: 231–256.

Dewulf, E.M., Cani, P.D., Claus, S.P., Fuentes, S., Puylaert, P.G., Neyrinck, A.M., *et al*. (2013) Insight into the prebiotic concept: lessons from an exploratory, double blind intervention study with inulin-type fructans in obese women. *Gut* **62**: 1112–1121.

Dörschug, M., Frank, R., Kalbitzer, H.R., Hengstenberg, W., and Deutscher, J. (1984) Phosphoenolpyruvate-dependent phosphorylation site in enzyme III^{glc} of the *Escherichia coli* phosphotransferase system. *Eur J Biochem* **144**: 113–119.

Duncan, S.H., Louis, P., Thomson, J.M., and Flint, H.J. (2009) The role of pH in determining the species composition of the human colonic microbiota. *Environ Microbiol* **11**: 2112–2122.

Duncan, S.H., Hold, G.L., Harmsen, H.J.M., Stewart, C.S., and Flint, H.J. (2002) Growth requirements and fermentation products of *Fusobacterium prausnitzii*, and a proposal to reclassify it as *Faecalibacterium prausnitzii* gen. Nov., comb. nov. *Int J Syst Evol Microbiol* **52**: 2141–2146.

Duncan, S.H., Scott, K.P., Ramsay, A.G., Harmsen, H.J., Welling, G.W., Stewart, C.S., and Flint, H.J. (2003) Effects of alternative dietary substrates on competition between human colonic bacteria in an anaerobic fermentor system. *Appl Environ Microbiol* **69**: 1136–1142.

El-Semman, I.E., Karlsson, F.H., Shoaie, S., Nookaew, I., Soliman, T.H., and Nielsen, J. (2014) Genome-scale metabolic reconstructions of *Bifidobacterium adolescentis* L2-32 and *Faecalibacterium prausnitzii* A2-165 and their interaction. *BMC Syst Biol* **8**: 41.

Fieulaine, S., Morera, S., Poncet, S., Mijakovic, I., Galinier, A., Janin, J., *et al*. (2002) X-ray structure of a bifunctional protein kinase in complex with its protein substrate HPr. *Proc Natl Acad Sci U S A* **99**: 13437–13441.

Fitzgerald, C.B., Shkoporov, A.N., Sutton, T.D.S., Chaplin, A.V., Velayudhan, V., Ross, R.P., and Hill, C. (2018) Comparative analysis of *Faecalibacterium prausnitzii* genomes shows a high level of genome plasticity and warrants separation into new species-level taxa. *BMC Genomics* **19**: 931.

Flint, H.J., Scott, K.P., Louis, P., and Duncan, S.H. (2012) The role of the gut microbiota in nutrition and health. *Nat Rev Gastroenterol Hepatol* **9**: 577–589.

Gassner, M., Stehlik, D., Schrecker, O., Hengstenberg, W., Maurer, W., and Rüterjans, H. (1977) The phosphoenolpyruvate-dependent phosphotransferase system of *Staphylococcus aureus*. 2. ^{1}H and ^{31}P-nuclear-magnetic-resonance studies on the phosphocarrier protein HPr, phosphohistidines and phosphorylated HPr. *Eur J Biochem* **75**: 287–296.

Gonzy-Tréboul, G., Zagorec, M., Rain-Guion, M.C., and Steinmetz, M. (1989) Phosphoenolpyruvate:sugar phosphotransferase system of *Bacillus subtilis*: nucleotide sequence of *ptsX*, *ptsH* and the 5′-end of *ptsI* and evidence for a *ptsHI* operon. *Mol Microbiol* **3**: 103–112.

Gurung, M., Li, Z., You, H., Rodrigues, R., Jump, D.B., Morgun, A., and Shulzhenko, N. (2020) Role of gut microbiota in type 2 diabetes pathophysiology. *EBioMedicine* **51**: 102590.

Halbedel, S., and Stülke, J. (2005) Dual phosphorylation of *mycoplasma pneumoniae* HPr by enzyme I and HPr kinase suggests an extended phosphoryl group susceptibility of HPr. *FEMS Microbiol Lett* **247**: 193–198.

Hayes, C.A., Dalia, T.N., and Dalia, A.B. (2017) Systematic genetic dissection of PTS in *vibrio cholerae* uncovers a novel glucose transporter and a limited role for PTS during infection of a mammalian host. *Mol Microbiol* **104**: 568–579.

Heinken, A., Khan, M.T., Paglia, G., Rodionov, D.A., Harmsen, H.J., and Thiele, I. (2014) Functional metabolic map of *Faecalibacterium prausnitzii*, a beneficial human gut microbe. *J Bacteriol* **196**: 3289–3302.

Heo, K., Park, Y.H., Lee, K.A., Kim, J., Ham, H.I., Kim, B.G., *et al*. (2019) Sugar-mediated regulation of a c-di-GMP phosphodiesterase in *vibrio cholerae*. *Nat Commun* **10**: 5358.

Hogema, B.M., Arents, J.C., Bader, R., Eijkemans, K., Yoshida, H., Takahashi, H., *et al*. (1998) Inducer exclusion in *Escherichia coli* by non-PTS substrates: the role of the PEP to pyruvate ratio in determining the phosphorylation state of enzyme IIA^{Glc}. *Mol Microbiol* **30**: 487–498.

Hustoft, T.N., Hausken, T., Ystad, S.O., Valeur, J., Brokstad, K., Hatlebakk, J.G., and Lied, G.A. (2017) Effects of varying dietary content of fermentable short-chain carbohydrates on symptoms, fecal microenvironment, and cytokine profiles in patients with irritable bowel syndrome. *Neurogastroenterol Motil* **29**: e12969.

Jang, C., Hui, S., Lu, W., Cowan, A.J., Morscher, R.J., Lee, G., *et al*. (2018) The small intestine converts dietary fructose into glucose and organic acids. *Cell Metab* **27**: 351–361.e353.

Kim, D., Paggi, J.M., Park, C., Bennett, C., and Salzberg, S. L. (2019) Graph-based genome alignment and genotyping with HISAT2 and HISAT-genotype. *Nat Biotechnol* **37**: 907–915.

Kim, E.J., Cho, Y.J., Chung, W.H., and Roe, J.H. (2020) The role of Rsv1 in the transcriptional regulation of genes involved in sugar metabolism for long-term survival. *FEBS J* **287**: 878–896.

Kim, H.M., Park, Y.H., Yoon, C.K., and Seok, Y.J. (2015) Histidine phosphocarrier protein regulates pyruvate kinase a activity in response to glucose in *Vibrio vulnificus*. *Mol Microbiol* **96**: 293–305.

Lee, C.R., Park, Y.H., Min, H., Kim, Y.R., and Seok, Y.J. (2019) Determination of protein phosphorylation by polyacrylamide gel electrophoresis. *J Microbiol* **57**: 93–100.

Liao, Y., Smyth, G.K., and Shi, W. (2014) featureCounts: an efficient general purpose program for assigning sequence reads to genomic features. *Bioinformatics* **30**: 923–930.

Lopez-Siles, M., Khan, T.M., Duncan, S.H., Harmsen, H.J., Garcia-Gil, L.J., and Flint, H.J. (2012) Cultured representatives of two major phylogroups of human colonic *Faecalibacterium prausnitzii* can utilize pectin, uronic acids, and host-derived substrates for growth. *Appl Environ Microbiol* **78**: 420–428.

Lopez-Siles, M., Martinez-Medina, M., Surís-Valls, R., Aldeguer, X., Sabat-Mir, M., Duncan, S.H., *et al*. (2016) Changes in the abundance of *Faecalibacterium prausnitzii* Phylogroups I and II in the intestinal mucosa of inflammatory bowel disease and patients with colorectal cancer. *Inflamm Bowel Dis* **22**: 28–41.

Love, M.I., Huber, W., and Anders, S. (2014) Moderated estimation of fold change and dispersion for RNA-seq data with DESeq2. *Genome Biol* **15**: 550.

Macfarlane, S., Quigley, M.E., Hopkins, M.J., Newton, D.F., and Macfarlane, G.T. (1998) Polysaccharide degradation by human intestinal bacteria during growth under multi-substrate limiting conditions in a three-stage continuous culture system. *FEMS Microbiol Ecol* **26**: 231–243.

Martín, R., Miquel, S., Benevides, L., Bridonneau, C., Robert, V., Hudault, S., *et al*. (2017) Functional characterization of novel *Faecalibacterium prausnitzii* strains isolated from healthy volunteers: a step forward in the use of *F. prausnitzii* as a next-generation probiotic. *Front Microbiol* **8**: 1226.

Mijakovic, I., Poncet, S., Galinier, A., Monedero, V., Fieulaine, S., Janin, J., *et al*. (2002) Pyrophosphate-producing protein dephosphorylation by HPr kinase/phosphorylase: a relic of early life? *Proc Natl Acad Sci U S A* **99**: 13442–13447.

Miquel, S., Martín, R., Bridonneau, C., Robert, V., Sokol, H., Bermúdez-Humarán, L.G., *et al*. (2014) Ecology and metabolism of the beneficial intestinal commensal bacterium *Faecalibacterium prausnitzii*. *Gut Microbes* **5**: 146–151.

Miquel, S., Martín, R., Rossi, O., Bermúdez-Humarán, L.G., Chatel, J.M., Sokol, H., *et al*. (2013) *Faecalibacterium prausnitzii* and human intestinal health. *Curr Opin Microbiol* **16**: 255–261.

Park, S., Park, Y.H., Lee, C.R., Kim, Y.R., and Seok, Y.J. (2016) Glucose induces delocalization of a flagellar biosynthesis protein from the flagellated pole. *Mol Microbiol* **101**: 795–808.

Park Y.H.Lee C.R.Choe M., and Seok Y.J. (2013) HPr antagonizes the anti-σ^{70} activity of Rsd in *Escherichia coli*. *Proc Natl Acad Sci U S A* **110**: 21142–21147.

Plumbridge, J. (2001) Regulation of PTS gene expression by the homologous transcriptional regulators, Mlc and NagC, in *Escherichia coli* (or how two similar repressors can behave differently). *J Mol Microbiol Biotechnol* **3**: 371–380.

Poncet, S., Soret, M., Mervelet, P., Deutscher, J., and Noirot, P. (2009) Transcriptional activator YesS is stimulated by histidine-phosphorylated HPr of the *Bacillus subtilis* phosphotransferase system. *J Biol Chem* **284**: 28188–28197.

Reizer, J., Romano, A.H., and Deutscher, J. (1993) The role of phosphorylation of HPr, a phosphocarrier protein of the phosphotransferase system, in the regulation of carbon metabolism in gram-positive bacteria. *J Cell Biochem* **51**: 19–24.

Reizer, J., Reizer, A., and Saier, M.H., Jr. (1995) Novel phosphotransferase system genes revealed by bacterial genome analysis--a gene cluster encoding a unique enzyme I and the proteins of a fructose-like permease system. *Microbiology (Reading)* **141**: 961–971.

Reizer, J., Novotny, M.J., Panos, C., and Saier, M.H. (1983) Mechanism of inducer expulsion in *Streptococcus pyogenes*: a two-step process activated by ATP. *J Bacteriol* **156**: 354–361.

Reizer, J., Bachem, S., Reizer, A., Arnaud, M., Saier, M.H., and Stülke, J. (1999) Novel phosphotransferase system genes revealed by genome analysis - the complete complement of PTS proteins encoded within the genome of *Bacillus subtilis*. *Microbiology (Reading)* **145**: 3419–3429.

Singh, K.D., Schmalisch, M.H., Stülke, J., and Görke, B. (2008) Carbon catabolite repression in *Bacillus subtilis*: quantitative analysis of repression exerted by different carbon sources. *J Bacteriol* **190**: 7275–7284.

Sokol, H., Pigneur, B., Watterlot, L., Lakhdari, O., Bermúdez-Humarán, L.G., Gratadoux, J.J., *et al*. (2008) *Faecalibacterium prausnitzii* is an anti-inflammatory commensal bacterium identified by gut microbiota analysis of Crohn disease patients. *Proc Natl Acad Sci U S A* **105**: 16731–16736.

Stülke, J., and Hillen, W. (1998) Coupling physiology and gene regulation in bacteria: the phosphotransferase sugar uptake system delivers the signals. *Naturwissenschaften* **85**: 583–592.

Tremaroli, V., and Bäckhed, F. (2012) Functional interactions between the gut microbiota and host metabolism. *Nature* **489**: 242–249.

Utzschneider, K.M., Kratz, M., Damman, C.J., and Hullar, M. (2016) Mechanisms linking the gut microbiome and glucose metabolism. *J Clin Endocrinol Metab* **101**: 1445–1454.

Wang, G., Sondej, M., Garrett, D.S., Peterkofsky, A., and Clore, G.M. (2000) A common interface on histidine-containing phosphocarrier protein for interaction with its partner proteins. *J Biol Chem* **275**: 16401–16403.

Wlodarska, M., Luo, C., Kolde, R., d'Hennezel, E., Annand, J.W., Heim, C.E., *et al*. (2017) Indoleacrylic acid produced by commensal Peptostreptococcus species suppresses inflammation. *Cell Host Microbe* **22**: 25–37e26.

Woting, A., and Blaut, M. (2016) The intestinal microbiota in metabolic disease. *Nutrients* **8**: 202.

Yoon, C.K., Kang, D., Kim, M.K., and Seok, Y.J. (2021) *Vibrio cholerae* FruR facilitates binding of RNA polymerase to the *fru* promoter in the presence of fructose 1-phosphate. *Nucleic Acids Res* **49**: 1397–1410.

Zoetendal, E.G., Rajilic-Stojanovic, M., and de Vos, W.M. (2008) High-throughput diversity and functionality analysis of the gastrointestinal tract microbiota. *Gut* **57**: 1605–1615.

Supporting Information

Additional Supporting Information may be found in the online version of this article at the publisher's web-site:

Appendix S1. Supporting Information.